Journal of Hazardous Materials 217–218 (2012) 11–18

Contents lists available at SciVerse ScienceDirect

Journal of Hazardous Materials

journal homepage: www.elsevier.com/locate/jhazmat

Cuprous oxide created on sepiolite: Preparation, characterization, and photocatalytic activity in treatment of red water from 2,4,6-trinitrotoluene manufacturing

Qingwei Zhu[a,b], Yihe Zhang[a,*], Fengzhu Lv[a], Paul K. Chu[c], Zhengfan Ye[d], Fengshan Zhou[a]

[a] State Key Laboratory of Geological Processes & Mineral Resources, National Laboratory of Mineral Materials, School of Materials Science and Technology, China University of Geosciences, Beijing 10083, China
[b] Beijing New Building Materials Public Limited Company, Beijing 102208, China
[c] Department of Physics & Materials Science, City University of Hong Kong, Kowloon, Hong Kong, China
[d] Department of Environmental Engineering, Key Laboratory of Water and Sediment Sciences of the Ministry of Education, Peking University, Beijing 100871, China

ARTICLE INFO

Article history:
Received 27 June 2011
Received in revised form
16 December 2011
Accepted 16 December 2011
Available online 16 January 2012

Keywords:
Cuprous oxide
Sepiolite
Red water
Photocatalysis

ABSTRACT

Cuprous oxide is firstly created on acidized sepiolite (AS) by a simple deposition method for photocatalytic degradation of the red water produced from 2,4,6-trinitrotoluene (TNT) manufacturing. X-ray diffraction (XRD), field-emission scanning electron microscopy (FE-SEM), ultraviolet-visible diffuse reflection absorptive spectroscopy (UV–vis/DRS), and Fourier transform infrared (FT-IR) spectroscopy are used to characterize the photocatalyst composites. Gas chromatography/mass spectrometry (GC/MS) is employed to determine the organic constituents in the red water. The results show that the cuprous oxide particles can be immobilized on the surface of the AS fibers and the structure of the AS is altered when cuprous oxide interacts with AS via chemical reactions besides physical adsorption. The AS improves the optical properties of cuprous oxide and red-shifts the band gap thereby enhancing the utilization of visible light. The Cu_2O/AS composites demonstrate excellent photocatalytic performance in the degradation of red water. 87.0% of red water can be photocatalytically degraded by Cu_2O/AS after illumined for 5 h and a majority of organic components of red water except 1,3,5-trinitrobenzene were degraded according to GC–MS analysis.

1. Introduction

Cuprous oxide is a promising p-type semiconductor photocatalyst having a narrow band gap of round 2.2 eV. It can be activated by irradiation of visible light which constitutes about 50% of sunlight. Hence, there have been many studies on the photocatalytic treatment of organic pollutants using cuprous oxide as the catalyst [1–6]. Unfortunately, cuprous oxide, especially those with nanoscale structure, is deactivated by photocorrosion easily [7] if it is not pretreated. Cuprous oxide is often combined with other oxide semiconductors, such as titanium oxide [8–11], zinc oxide [12,13], and tungsten trioxide [14], to improve the optical properties and/or stability. Some porous materials have also used as the support for cuprous oxide to promote the photocatalytic performance. Among these materials, silicon oxide [15], aluminum oxide [16], and activated carbon [17] are commonly used. The high specific surface area is the main consideration. Moreover, porous minerals are simple and cheap. They have been widely applied as carriers for some functional materials. In our previous study, Cu_2O–ZnO was immobilized on diatomite and its photocatalytic activity with regard to the degradation of red water from 2,4,6-trinitrotoluene (TNT) manufacturing was improved [18].

Sepiolite, a hydrated magnesium silicate, is one of common porous clay minerals with a typical structural formula $Mg_4Si_6O_{15}(OH)_2{\cdot}6H_2O$ [19] in the half-unit cell having a fibrous morphology and intracrystalline channels. It has a large surface area (more than 200 $m^2\,g^{-1}$) [20] as well as high chemical and mechanical stability. Therefore, sepiolite has been used to remove organic contaminants in industry [19,21–23]. It has also been used as an effective carrier for TiO_2 and ZnO in the photocatalytic treatment of pollutants [24–29]. However, the use of other photocatalysts like Cu_2O on sepiolite has not been reported.

In this study, acid activated sepiolite (AS) serves as the support for cuprous oxide and simple precipitation is utilized to put Cu_2O on the acidized sepiolite. The structural characteristics and photocatalytic properties of these composites in the treatment of red water

* Corresponding author. Tel.: +86 10 82323344; fax: +86 10 82323344.
E-mail addresses: zyh@cugb.edu.cn, bjzhqw@sina.com (Y. Zhang).

0304-3894/$ – see front matter © 2011 Elsevier B.V. All rights reserved.
doi:10.1016/j.jhazmat.2011.12.053

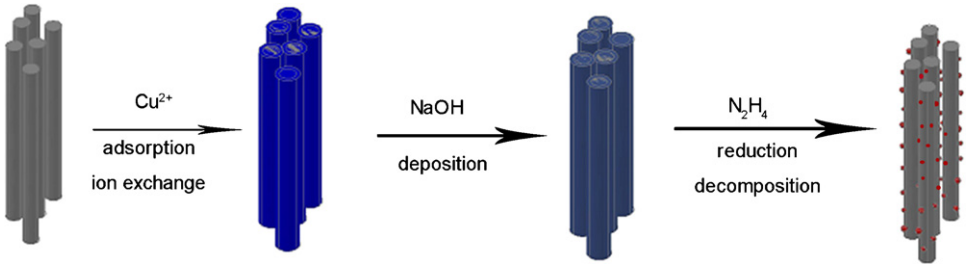

Scheme 1. Schematic presentation for the preparation procedure of Cu_2O/AS.

produced from TNT manufacturing are studied and our results suggest that these unique composites are promising photocatalysts for degradation of red water.

2. Experimental

2.1. Preparation of Cu_2O/sepiolite composites

Sepiolite obtained from Hebei Hongli Sepiolite Fiber Co., Ltd. (Hebei Province, China) was used as the supporting materials. It was pretreated with acid to enable the fibers to disperse uniformly and increase the specific surface area. The pretreatment procedure is as follows: (1) the sepiolite was put into deionized water (mass ratio of sepiolite and water was 1:10) and stirred for 30 min, then kept it unstirred for 30 min. After that, the suspension was centrifuged and the deposit in the bottom was removed. This procedure was repeated for three times. (2) 300 g of the sepiolite washed by deionized water was conditioned in 500 mL of 1.0 mol L^{-1} nitric acid and stirred for 3 h at room temperature. (3) The acidized suspension was centrifuged and rinsed with deionized water 15 times to remove any trace of the acid. (4) The solid was dried for 5 h at 60 °C.

The Cu_2O/AS samples were prepared as shown in Scheme 1. 5.0 g of the acidic sepiolite (AS) powder was immersed in 50.0 mL of 0.5 mol L^{-1} copper nitrate solution and 3 mL of 5% (W/V) poly-vinylpyrrolidone (average molecular weight = 27,000–33,000, PK30). The suspension was ultrasonicated for 1 h to get more impregnation of Cu^{2+} on the AS. Then 50 mL of 1.0 mol L^{-1} sodium hydroxide solution was added to the above suspension under vigorous stirring. After 7.0 mL of 1.0 mol L^{-1} hydrate hydrazine was added and stirred at 80 °C for 10 min, the precipitate was filtrated and washed with deionized water and absolute ethanol several times to remove unwanted impurities. The product was dried in a vacuum desiccator at 80 °C for 2 h. This sample was designated ASC-5.

For comparison, 50 mL of the copper nitrate solution with different concentrations (0.05, 0.1, 0.2, 0.3, and 0.4 mol L^{-1}) were used to obtain Cu_2O/AS samples with different loadings. Accordingly, the concentrations of sodium hydroxide were 0.1, 0.2, 0.4, 0.6, and 0.8 mol L^{-1} and the doses of hydrate hydrazine were 0.7, 1.4, 2.4, 4.2, and 5.6 mL. The obtained samples were labeled as ASC-0.5, ASC-1, ASC-2, ASC-3, and ASC-4, respectively.

2.2. Characterization of Cu_2O/AS composites

Field-emission scanning electron microscopy (FE-SEM, Hitachi S-4500) was performed at 15 kV to determine the microstructures and morphologies of the composites. All the samples were sputter-coated with a thin layer of carbon before microscopic observation. The specific surface area (S_{BET}) of the samples was determined by an automated surface area and pore size analyzer (Autosorb-1, Quantachrome, USA) based on nitrogen adsorption. The crystal structure of the synthesized particles was determined by X-ray diffraction (XRD, Rigaku D/Max-2000) using Cu K_α radiation (2 kV rotating anode, λ = 1.54056 Å). The samples were scanned from 10° to 90° at a scanning rate of 8° min^{-1}. The Fourier transform infrared (FT-IR) spectra of the samples were acquired on a PerkinElmer Spectrum 100 FT-IR spectrophotometer in the 4000–400 cm^{-1} range. The samples were made into potassium bromide pellets. The ultraviolet–visible diffuse reflection absorptive spectra (UV–vis/DRS) were obtained on a Lambda-900 UV/vis/NIR spectrometer (PerkinElmer, USA) equipped with an integration sphere at room temperature. The organic composition of the red water was determined by a Gas Chromatography–Mass Spectrometry (GC–MS, GC6890N/MSD5973, Agilent Technologies, USA). A DB-35 MS capillary column with an inner diameter of 0.25 mm and length of 60 m was used in the separation system. Helium was introduced as the carrier gas at a flow rate of 1.0 mL/min. 1.0 μL of the sample was injected into the GC–MS operated from 40 to 280 °C at a programmable rate of 2.0 °C min^{-1}.

2.3. Photocatalytic treatment of red water

The red water produced from TNT manufacturing was obtained from Dongfang Chemical Corporation (Hubei Province, China). The photocatalytic experiments were carried out in a reactor equipped with water cooling, magnetic stirring and a mercury tungsten blended lamp (500 W) positioned about 12.5 cm above the solution surface. Because the original red water is too dense and dark, it would be hardly efficiently photocatalytically treated if it was not diluted. In the typical photocatalytic experiment, 1.0 g of the photocatalyst was added to 200 mL of red water diluted 200 times using deionized water. The photocatalyst was dispersed under ultrasonic vibration for 10 min in the absence of light. At the end of the experiment, the suspension was separated by filtration. The photocatalytic degradation rate of red water was determined on an HP Agilent 8453 UV–visible spectrophotometer (Hewlett Packard).

3. Results and discussion

3.1. XRD patterns of nanocomposites

The changes in the acidic sepiolite (AS) and Cu_2O/AS composite materials were monitored by XRD. Fig. 1 depicts the XRD patterns from 10° to 80° acquired from the raw sepiolite and AS. Some peaks weaken or vanish and some new peaks appear. It demonstrates that the crystalline structure changes significantly after sepiolite is treated with nitric acid and it results from magnesium ions being replaced by hydrogen in sepiolite skeleton. A new phase occurs. And in its structure unit, two Si–OH groups substitutes a –Si–O–Mg–O–Si– group of original sepiolite [30].

Fig. 2 illustrates some differences in their crystalline structures of different Cu_2O loadings on the AS. Sepiolite exhibits the anhydride according to Fig. 2(a). The sepiolite structure consists of an individual fiber with $Mg_8Si_{12}O_{30}(OH)_4$ as the fundamental structure according to the JCPDS card No. 26-1227. In Fig. 2(b)–(g), according to the JCPDS card No.05-0667, four other characteristic

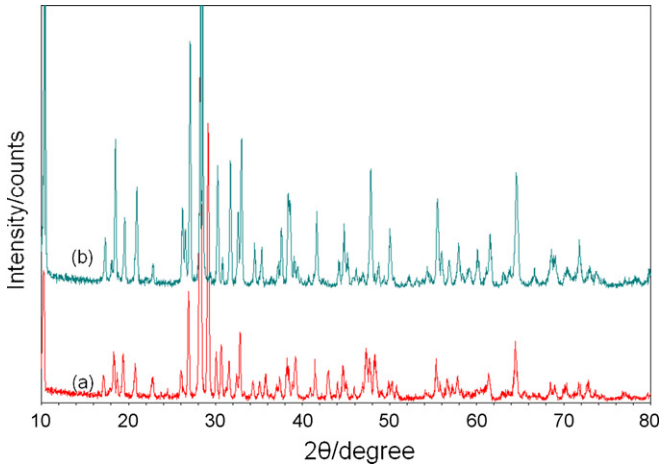

Fig. 1. XRD patterns of (a) raw sepiolite and (b) acidized sepiolite.

peaks are observed at 2θ values of 36.5°, 42.3°, 61.6°, and 73.5°, corresponding to the crystal planes of (1 1 1), (2 0 0), (2 2 0), and (3 1 1) of crystalline cuprous oxide, respectively. The intensity increases with larger loading of cuprous oxide. The results imply that cuprous oxide with the cubic structure is stably loaded on the surface of sepiolite. It is interesting that in Fig. 2(d)–(g) a new peak in 12.6° belonging to neither sepiolite nor cuprous oxide emerges and the intensity is attenuated with increasing copper concentration. This may be attributed to ion exchange between copper and hydrogen. Parts of copper ion superseding hydrogen ion were not reduced into Cu_2O. A new sepiolite was formed. When the Cu concentration is low (0.05 and 0.1 mol L^{-1}), the peak at 12.6° cannot be observed because ion exchange is not enough to change the structure of sepiolite. However, if the Cu^{2+} concentration is too high (0.5 mol L^{-1}), besides ion exchange, more copper ions were adsorbed on the surface of the fibers of sepiolite. Thus, a mass of cuprous oxide is immobilized on the sepiolite as evidenced by the change in the diffraction of the composites. On the other hand, a decrease in the sepiolite peak intensity occurs due to the imperfect crystalloid by disconnecting the fiber unit [31]. Furthermore, there are no impurity peaks like copper and copper oxide shown in the patterns, which illustrate the high purity of the prepared cuprous oxide.

According to Scherrer formula, the crystalline sizes of Cu_2O particles in ASC-0.5, 1, 2, 3, 4, 5 are estimated at 43, 38, 34, 35, 31, 33 nm, respectively. The particle sizes are almost uniform, demonstrating the stability of the crystalline size of Cu_2O synthesized under the same conditions. And Cu_2O crystals with such big size cannot be incorporated within layers of AS support but only immobilized on the surface of sepiolite fibers.

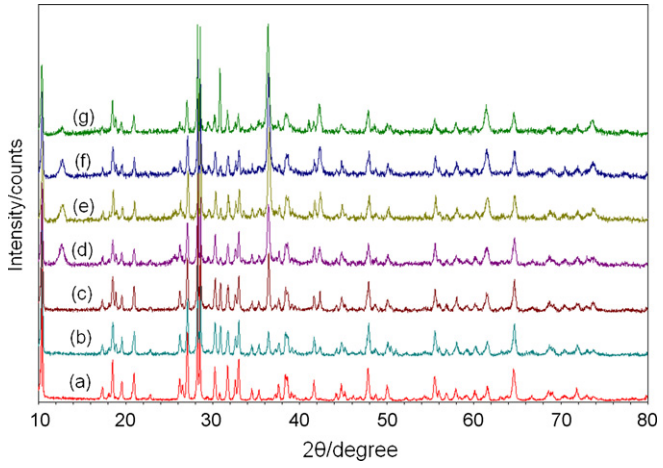

Fig. 2. XRD patterns of acidized sepiolite and different Cu_2O/AS: (a) AS, (b) ASC-0.5, (c) ASC-1, (d) ASC-2, (e) ASC-3, (f) ASC-4, and (g) ASC-5.

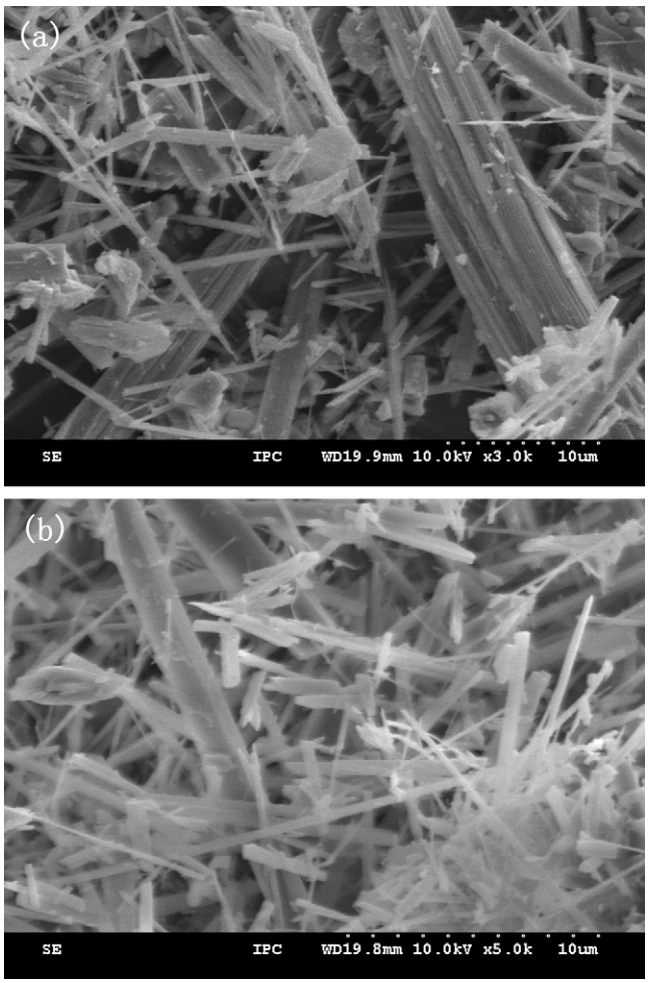

Fig. 3. SEM images of (a) raw sepiolite and (b) acidized sepiolite.

3.2. SEM and BET surface area of nanocomposites

Sepiolite is a clay mineral with a fibrous morphology. The changes occurring on the surface of the AS demonstrate whether the cuprous oxide is supported on AS. The SEM images provide information about the morphology of the composite materials obtained from the acid activated sepiolite samples (Fig. 3). Fig. 3(a) is the SEM image of the raw sepiolite and reveals stone-like aggregation made up of lots of fibers with a size of about 100 nm and a large specific surface area (S_{BET} = 51.147 $m^2\,g^{-1}$). When sepiolite is processed with nitric acid, these fibers are cleaved (Fig. 3b) and their specific surface areas increase slightly to 57.118 $m^2\,g^{-1}$. Careful examination of the SEM images of the Cu_2O/AS composites in Fig. 4 discloses that more cuprous oxide particles with a diameter of 100–500 nm are immobilized on the acid-treated sepiolite as the copper nitrate concentration increased. And the Cu_2O particles aggregate slightly. The specific surface area of Cu_2O/AS are measured and listed in Table 1. The reduction observed from the specific surface area gains with the increasing loadings of Cu_2O, which is associated with adsorption of slightly aggregating cuprous oxide by the sepiolite mineral.

Scheme 1 summarizes our approach to prepare the photocatalyst composites. Cu^{2+} are firstly adsorbed on the acidized sepiolite fibers and/or ion-exchange occurs with H^+ in the sepiolite. It then

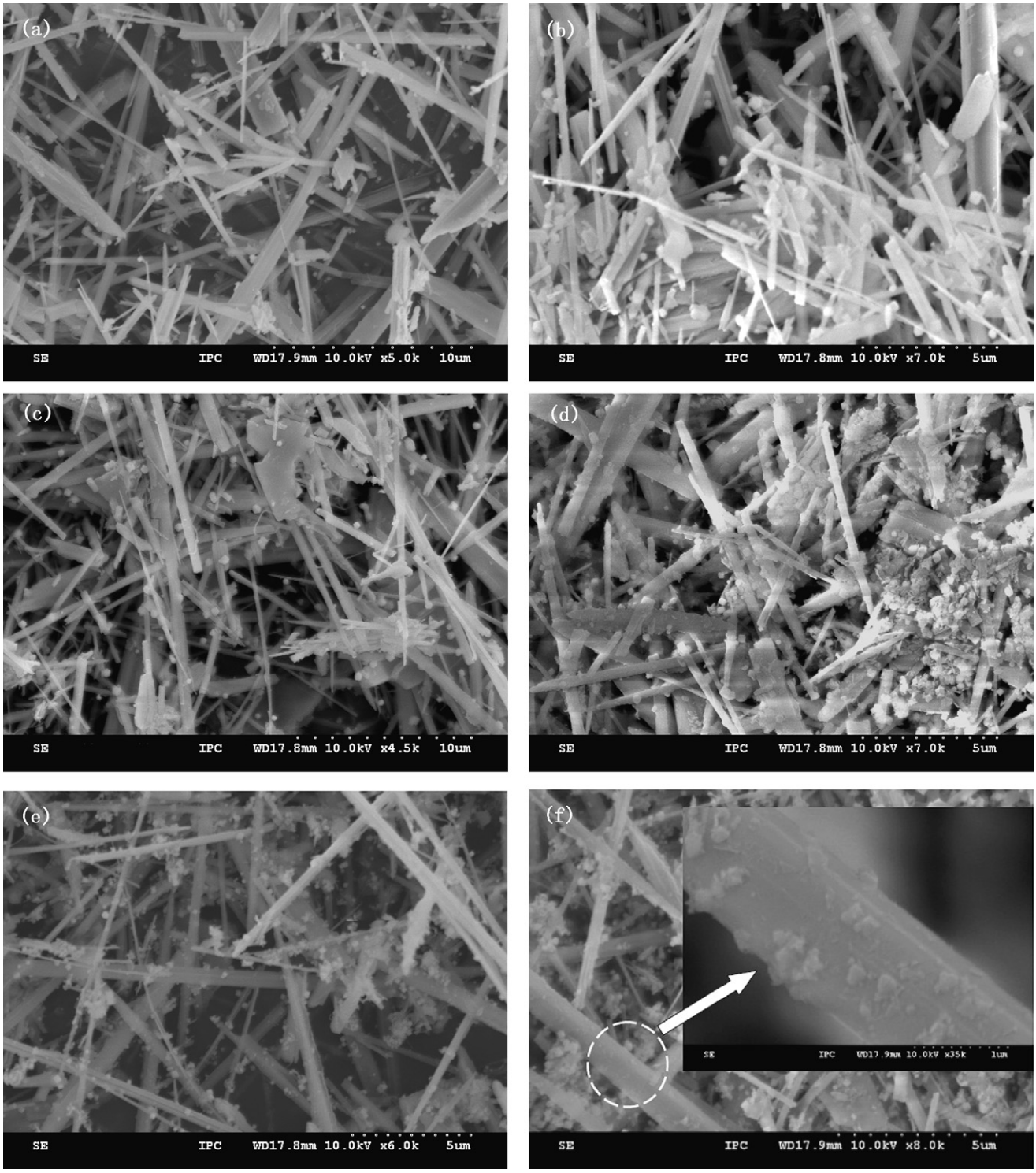

Fig. 4. SEM images of different Cu_2O/AS samples: (a) ASC-0.5, (b) ASC-1, (c) ASC-2, (d) ASC-3, (e) ASC-4, and (f) ASC-5.

Table 1
The specific surface areas of samples (S_{BET}) and the photocatalytic degradation rate of red water by various samples after irradiated for 5 h (Dg).

Sample	AS	ASC-0.5	ASC-1	ASC-2	ASC-3	ASC-4	ASC-5
S_{BET} ($m^2\ g^{-1}$)	57.118	56.095	54.143	44.348	39.700	33.654	33.277
Dg (%)	–	64.4	71.7	76.3	83.6	85.5	87.0

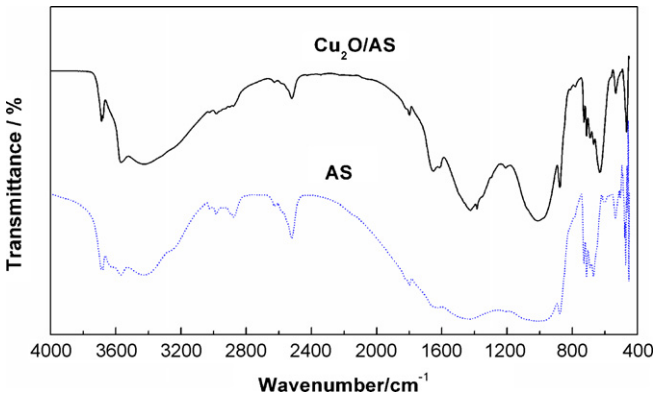

Fig. 5. FT-IR spectra of (a) acidized sepiolite (AS) and (b) Cu_2O/AS (ASC-5).

reacts with OH^- to generate $Cu(OH)_2$ and deposits on the surface of the sepiolite fibers when NaOH is added. When N_2H_4 is introduced, $Cu(OH)_2$ is reduced to CuOH and immediately decomposes into Cu_2O immobilized on the sepiolite fibers by adsorption due to the instability of CuOH. The mechanism is in agreement with the experimental result [the insert of Fig. 4(f)].

3.3. FT-IR analyses of nanocomposites

To further characterize the structure of Cu_2O/AS, ASC-5 is analyzed using FT-IR. As shown in Fig. 5, bands at 3760–3580 cm^{-1} attributed to the stretching vibration of Mg–OH in the Mg–O octahedron become weak. It suggests that Mg–OH is destroyed during acid treatment of sepiolite. The peak at 3430 cm^{-1} is attributed to the presence of zeolitic water in the mineral and the weak stretching vibrations of –OH groups located in the Mg–O octahedron appears at approximately 1660 cm^{-1} due to the loss of water during the acid treatment. On the other hand, the bending vibration of –OH groups on the sepiolite surface and the stretching vibrations of Si–O–Si in the Si–O tetrahedron at 1400 and 1010 cm^{-1} in AS are weak but strengthened in the Cu_2O/sepiolite composites. It may be caused by the recovery of the AS structure when Cu^{2+} ion exchanges with the sepiolite. This is supported by the XRD results. Furthermore, as shown in Fig. 5b, the strong band at 630 cm^{-1} originates from the stretching vibrations of Cu–O in Cu_2O. And the spectrum confirms the absence of cupric oxide which has a fingerprint band at around 530 cm^{-1}.

3.4. UV–vis/DRS and band gaps of composites

The ultraviolet–visible diffuse reflectance absorptive spectra (UV–vis DRS) are used to characterize the optical absorbance of the Cu_2O/AS composite. Here, we analyze the UV–vis DRS of ASC-5 and estimate the band gap. The absorption spectrum of ASC-5 is shown in Fig. 6(a). An absorption edge exists at around 650 nm. Cuprous oxide is loaded on sepiolite and the absorption edge appears red-shifted to some extent, implying improved absorption of visible light. On the other hand, ASC-5 exhibits a lower absorbance in the UV range than pure Cu_2O prepared with the similar approach due to the smaller light absorption of sepiolite compared to cuprous oxide. However, ASC-5 can absorb more visible light relative to pure Cu_2O, revealing that AS promotes the utilization of visible light by Cu_2O.

The optical band gap energy can be estimated using the following equation for a semiconductor with a direct band gap [32]:

$$\alpha h\nu = C(h\nu - E_g)^{\frac{1}{2}} \quad (1)$$

where C is a constant which does not depend on the photon energy, α is the absorbance coefficient, and E_g is the band gap energy.

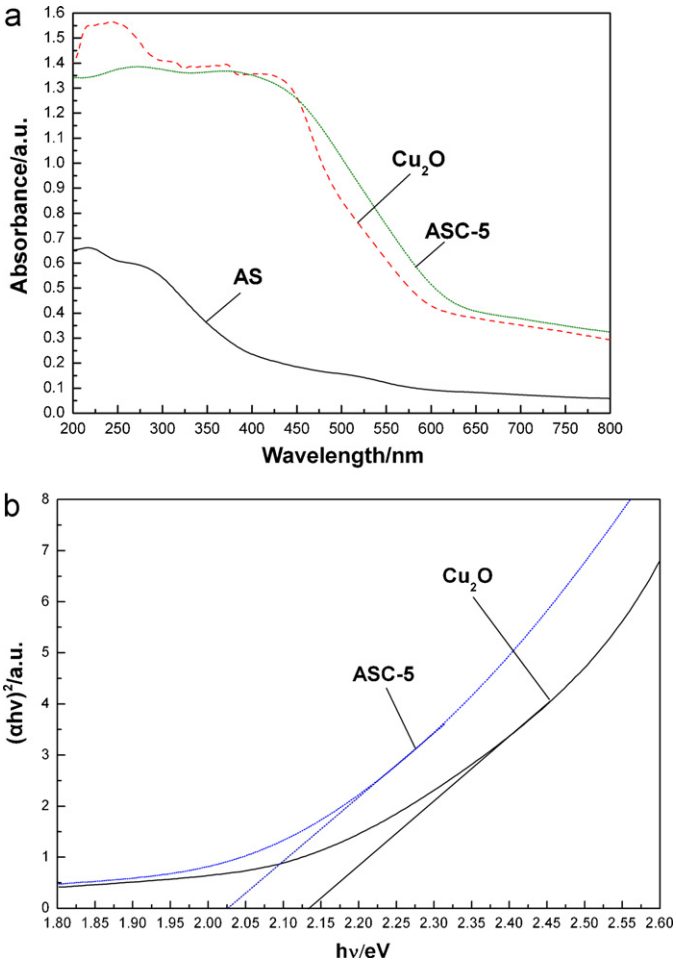

Fig. 6. (a) UV–vis DRS of pure Cu_2O, AS and ASC-5 and (b) plots of $(\alpha h\nu)^2$ versus $h\nu$ of Cu_2O and ASC-5.

The band gap is estimated from the intercepts of the tangents to the $(\alpha h\nu)^2$ versus photon energy ($h\nu$) plots. Fig. 6(b) depicts the plots of $(\alpha h\nu)^2$ versus $h\nu$ for pure Cu_2O and ASC. The direct band gaps of ASC-5 and pure Cu_2O are estimated to be 2.02 and 2.13 eV, respectively. The slight red shift in the direct band gap occurs when cuprous oxide is immobilized on the AS. It is attributed to the effects of the carrier AS on the crystal structure. Because of the influence of the interface of the AS on the growth direction of the crystals, the active dominant facet of cuprous oxide is promoted and the surface optical properties of the crystals are improved [18]. Consequently, the minimum activate energies of Cu_2O crystals are lowered and their sensitivity of visible light is enhanced.

3.5. Photocatalytic activity of nanocomposites in treatment of red water

The photocatalytic activity of Cu_2O loaded on the acid-treated sepiolite is assessed by monitoring the degradation of red water from TNT manufacturing in an aqueous solution under visible light irradiation. In our previous study, the direct photolysis rate of red water is 4.91% when irradiated by visible light for 6 h in the absence of photocatalysts, suggesting that photolysis was negligible [18].

Red water from TNT manufacturing has complex constituents and it is very difficult to determine the photocatalytic degradation rate. In this study, we determine the degradation of red water by

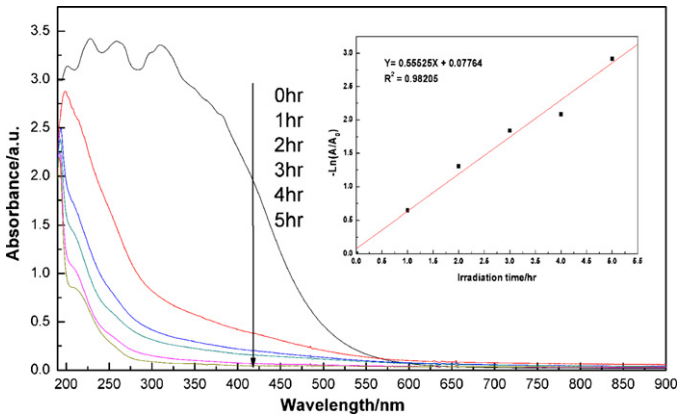

Fig. 7. UV–vis spectra of the remaining red water treated by ASC-5 in different time.

measuring the UV–vis absorbance and calculate by the following equation:

$$D(\%) = \frac{C_0 - C_t}{C_0} \times 100 = \frac{A_0 - A_t}{A_0} \times 100 \quad (2)$$

Here C_0, C_t are the concentration of initial and residual red water and A_0, A_t are their corresponding absorbance in the wavelength of 420 nm, respectively.

Fig. 7 depicts the UV–vis results obtained from the red water degraded by sample ASC-5, demonstrating that the red water has been effectively photocatalytically degraded. At the wavelength of 420 nm, the calculated degradation rate of red water is 87.0% after the irradiation of 5 h. It is higher than the Cu_2O/diatomite sample (33.3%) prepared by the same method in our previous work [18]. The integral form of the pseudo-first-order rate equation is generally expressed as follows:

$$-Ln\ \frac{A_t}{A_0} = k \times t \quad (3)$$

where A_0 is the initial absorbance of red water and A_t is the residual one. k is the observed first-order rate constant. The insert of Fig. 7 shows an observed first-order rate constant (k) of 0.55525 h^{-1} and a correlation coefficient of 0.98205. From these data, it appears to be in agreement with the experimental data on the photodegradation of red water and there is a big observed first-order reaction rate. It implies that red water can be efficiently degraded by Cu_2O/AS composite photocatalysts.

To further investigate the degradation of red water, GC–MS is conducted to detect the remaining components in the red water treated by the photocatalyst. The mass spectra are utilized to identify the components according to the NIST05 mass spectral library database. Fig. 8 shows the GC–MS analysis results before and after treatment with ASC-5. Over 12 components, such as TNT, 3,5-dinitro-p-toluidine, 2,6-dinitrotoluene, 2,5-dinitrotoluene, 2-nitrotoluene, 4-nitrotoluene, 3-methyl-6-nitrobenzoic acid, 5-methyl-2-nitrophenol, 3-methyl-2-nitrophenol, 2-methyl-3,5-dinitrophenol, 2,4-dinitrotoluene, and 1,3,5-trinitrobenzene, exist in the initial red water, but only 1,3,5-trinitrobenzene can be detected in the red water after photocatalytic degradation by sample ASC-5. Hence, a majority of organic molecules have been degraded. When photocatalyst Cu_2O absorbs the radiation the visible lights, pairs of negative-electron (e^-), and positive-hole (h^+) pair will be produced. And the hydroxyl radicals ($OH^\bullet$) are generated by the reaction between holes (h^+) and adsorbed OH^-. The organic pollutants react with OH· and are oxidized into CO_2, H_2O, or smaller molecules to achieve photocatalytic degradation. In this work, organic molecules in the red water reacted with OH· under the irradiation of the visible light, and were oxidized into CO_2 and H_2O partially or entirely.

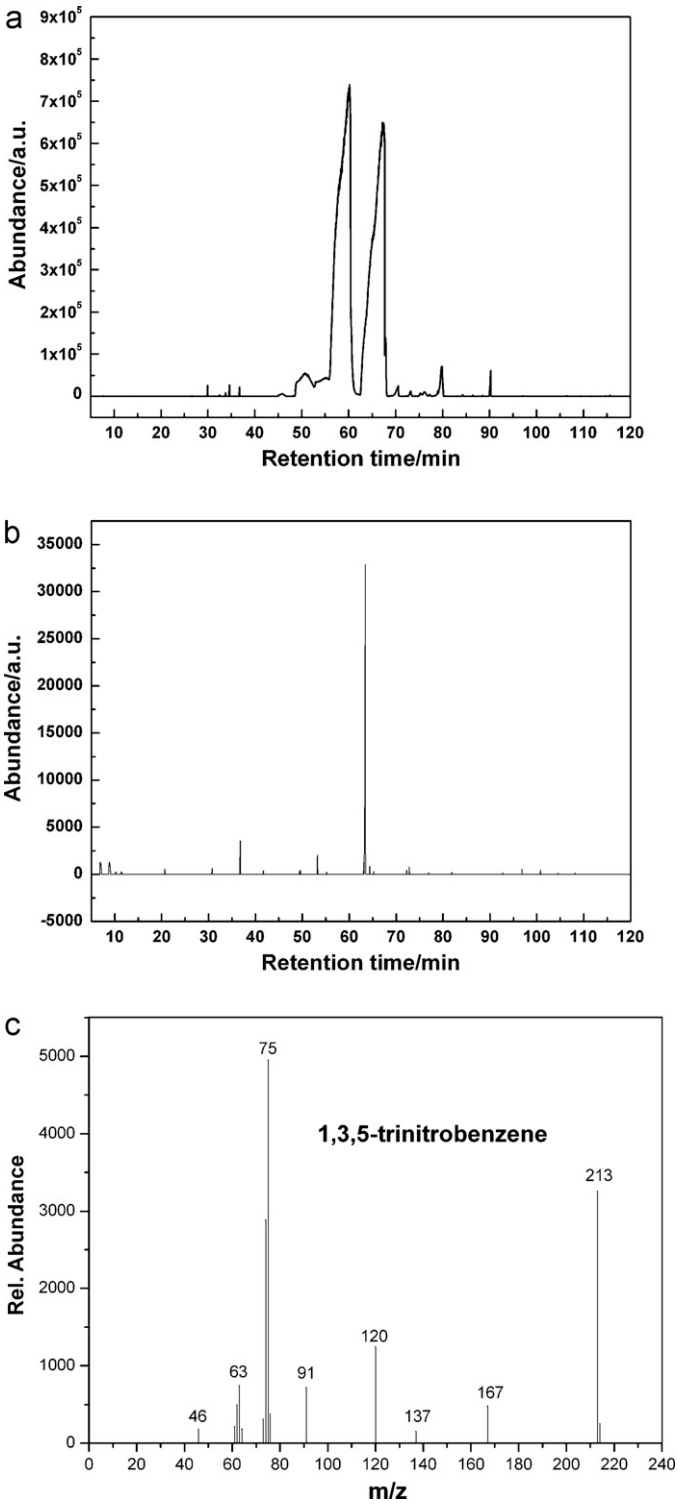

Fig. 8. Gas chromatography of red water (a) before and (b) after treated by ASC-5, and (c) the mass spectrum of the compounds with the retention time of 63.5 min.

The photocatalytic degradation of red water using samples with different Cu_2O loadings is shown in Fig. 9 and Table 1. It reveals the excellent photocatalytic activity of the sample ASC-3, ASC-4, and ASC-5 and a slight increase among them. Our data suggest that ASC-5 is the comparatively optimal sample.

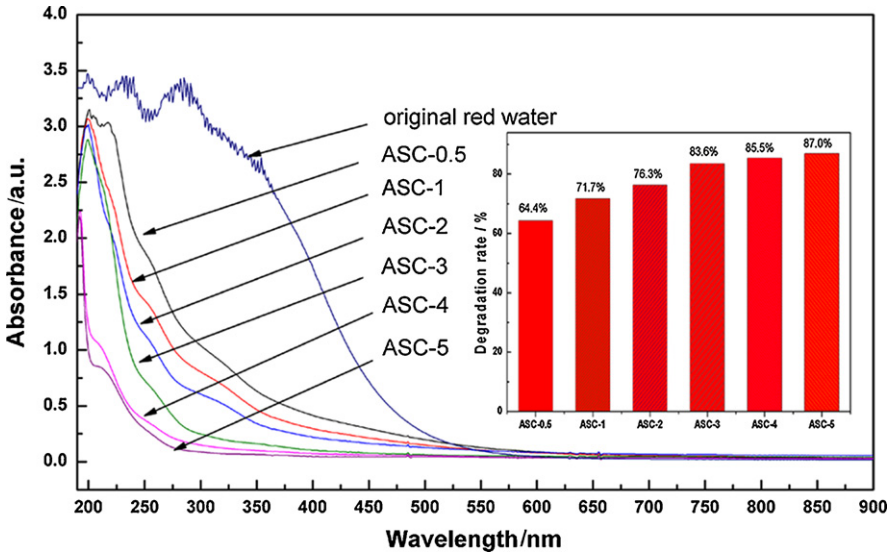

Fig. 9. UV–vis spectra of the remaining red water treated for 5 h by different photocatalysts.

4. Conclusions

Cu_2O/AS composites have been firstly prepared successfully by a simple deposition method. The acid treated sepiolite (AS) fiber is an excellent carrier of Cu_2O particle and improves efficiently the photocatalytic activity of Cu_2O. XRD patterns illustrate that the AS structure changes when cuprous oxide interacts with the AS by chemical reactions besides physical adsorption. UV–vis DRS analysis reveals that AS improves the optical properties of cuprous oxide and red-shifts the band gap, thereby ameliorating the utilization of visible light. The Cu_2O/AS samples have excellent photocatalytic performance in the degradation of red water from TNT manufacturing. In the photocatalytic treatment of red water, a majority of organic molecules except 1,3,5-trinitrobenzene are degraded efficiently as revealed by GC–MS. The Cu_2O/sepiolite composites are very promising and competitive photocatalyst candidates in the treatment of red water from TNT manufacturing.

Acknowledgment

This study was supported by the Foundational Research Funds for the Central Universities (2010ZD08, 2011PY0179, 2011PY0180, 2011PY0181), and the open foundation of National Laboratory of Mineral Materials of China University of Geosciences (Grant Nos. 519002310062, 08A004, 08A006).

References

[1] S. Kakuta, T. Abe, Photocatalytic activity of Cu_2O nanoparticles prepared through novel synthesis method of precursor reduction in the presence of thiosulfate, Solid State Sci. 11 (2009) 1465–1469.
[2] X. Zhang, J. Song, J. Jiao, X. Mei, Preparation photocatalytic activity of cuprous oxides, Solid State Sci. 12 (2010) 1215–1219.
[3] H. Yang, J. Ouyang, A. Tang, Y. Xiao, X. Li, X. Dong, Y. Yu, Electrochemical synthesis and photocatalytic property of cuprous oxide nanoparticles, Mater. Res. Bull. 41 (2006) 1310–1318.
[4] H. Zhu, J. Zhang, C. Li, F. Pan, T. Wang, B. Huang, Cu_2O thin films deposited by reactive direct current magnetron sputtering, Thin Solid Films 517 (2009) 5700–5704.
[5] A. Tang, Y. Xiao, J. Ouyang, S. Nie, Preparation, photo-catalytic activity of cuprous oxide nano-crystallites with different sizes, J. Alloys Compd. 457 (2008) 447–451.
[6] J.Y. Ho, M.H. Huang, Synthesis of submicrometer-sized Cu_2O crystals with morphological evolution from cubic to hexapod structures and their comparative photocatalytic activity, J. Phys. Chem. C 113 (2009) 14159–14164.
[7] L. Huang, F. Peng, H. Yu, H.J. Wang, Preparation of cuprous oxides with different sizes and their behaviors of adsorption visible-light driven photocatalysis and photocorrosion, Solid State Sci. 11 (2009) 129–138.
[8] Y. Bessekhouad, D. Robert, J.-V. Weber, Photocatalytic activity of Cu_2O/TiO_2, Bi_2O_3/TiO_2 and $ZnMn_2O_4/TiO_2$ heterojunctions, Catal. Today 101 (2005) 315–321.
[9] L. Huang, F. Peng, H. Wang, H. Yu, Z. Li, Preparation and characterization of Cu_2O/TiO_2 nano–nano heterostructure photocatalysts, Catal. Commun. 10 (2009) 1839–1843.
[10] W. Siripala, A. Ivanovskaya, T.F. Jaramillo, S.H. Baeck, E.W. McFarland, A Cu_2O–TiO_2 heterojunction thin film cathode for photoelectrocatalysis, Sol. Energ. Mater. Sol. C 77 (2003) 229–237.
[11] J. Li, L. Liu, Y. Yu, Y. Tang, H. Li, F. Du, Preparation of highly photocatalytic active nano-size TiO_2–Cu_2O particle composites with a novel electrochemical method, Electrochem. Commun. 6 (2004) 940–943.
[12] N. Helaïli, Y. Bessekhouad, A. Bouguelia, M. Trari, p-Cu_2O/n-ZnO heterojunction applied to visible light Orange II degradation, Sol. Energy 84 (2010) 1187–1192.
[13] C. Xu, L. Cao, G. Su, W. Liu, H. Liu, Y. Yu, X. Qu, Preparation of ZnO/Cu_2O compound photocatalyst and application in treating organic dyes, J. Hazard. Mater. 176 (2010) 807–813.
[14] C.C. Hua, J.N. Nian, H. Teng, Electrodeposited p-type Cu_2O as photocatalyst for H_2 evolution from water reduction in the presence of WO_3, Sol. Energ. Mater. Sol. C 92 (2008) 1071–1076.
[15] W. Chang, Y. Shen, A. Xie, W. Tong, Preparation of Al_2O_3-supported nano-Cu_2O catalysts for the oxidative treatment of industrial wastewater, Russian J. Phys. Chem. A 83 (2009) 2308–2312.
[16] X. Zhang, D. Zhang, X. Ni, H. Zheng, Synthesis and optical properties of Cu_2O/SiO_2 composite films via gamma-irradiation route, Mater. Lett. 61 (2007) 248–250.
[17] Z. Li, C.M. Wen, H.Y. Zheng, K.C. Xie, Effects of the active carbon surface properties on the structure and catalytic activity of Cu_2O/AC catalyst chemical, Chem. J. Chin. U. 31 (2010) 145–152.
[18] Q.W. Zhu, Y.H. Zhang, F.S. Zhou, F.Z. Lv, Z.F. Ye, F.D. Fan, P.K. Chu, Preparation and characterization of Cu_2O–ZnO immobilized on diatomite for photocatalytic treatment of red water produced from manufacturing of TNT, Chem. Eng. J. 171 (2011) 61–68.
[19] G. Rytwo, D. Tropp, C. Serban, Adsorption of diquat, paraquat and methyl green on sepiolite: experimental results and model calculations, Appl. Clay Sci. 20 (2002) 273–282.
[20] J. Menesi, L. Korosi, E. Bazsoa, V. Zollmer, A. Richardt, I. Dekany, Photocatalytic oxidation of organic pollutants on titania/clay composites, Chemosphere 70 (2008) 538–542.
[21] E. Eren, B. Afsin, Investigation of a basic dye adsorption from aqueous solution onto raw and pre-treated sepiolite surfaces, Dyes Pigments 73 (2007) 162–167.
[22] M. Alkan, M. Doğan, Y. Turhan, Ö. Demirbaş, P. Turan, Adsorption kinetics and mechanism of maxilon blue 5G dye on sepiolite from aqueous solutions, Chem. Eng. J. 139 (2008) 213–223.
[23] A. Özcan, ÖzcanF A.S., Adsorption of Acid Red 57 from aqueous solutions onto surfactant-modified sepiolite, J. Hazard. Mater. B125 (2005) 252–259.
[24] P. Aranda, R. Kun, M.A. Martín-Luengo, S. Letaïef, I. Dékány, E. Ruiz-Hitzky, Titania-sepiolite nanocomposites prepared by a surfactant templating colloidal route, Chem. Mater. 20 (2008) 84–91.

[25] M. Uğurlu, M.H. Karaoğlu, TiO_2 supported on sepiolite: preparation, structural and thermal characterization and catalytic behavior in photocatalytic treatment of phenol and lignin from olive mill wastewater, Chem. Eng. J. 166 (2010) 859–867.
[26] C. Knapp, F.J. Gil-Llambías, M. Gulppi-Cabra, J. Avila, P. Blanco, Phase distribution in titania–sepiolite catalyst supports prepared by different methods, J. Mater. Chem. 7 (1997) 1641–1645.
[27] A. Neren Ökte, Elçin Sayınsöz, Characterization and photocatalytic activity of TiO_2 supported sepiolite catalysts, Sep. Purif. Technol. 62 (2008) 535–543.
[28] W.G. Xu, S.F. Liu, S.X. Lu, S.Y. Kang, Y. Zhou, H.F. Zhang, Photocatalytic degradation in aqueous solution using quantum-sized ZnO particles supported on sepiolite, J. Colloid Interf. Sci. 351 (2010) 210–216.
[29] D. Karamanis, A.N. Ökte, E. Vardoulakis, T. Vaimakis, Water vapor adsorption and photocatalytic pollutant degradation with TiO_2-sepiolite nanocomposites, Appl. Clay Sci. 53 (2011) 181–187.
[30] S. Li, L. Luo, J. Guo, F. Li, Modification and recent application of sepiolite as a novel catalytic material, J. Nat. Gas Chem. 10 (2001) 338–348.
[31] S.M. Jung, P. Grange, Characterization of the surface hydroxyl properties of sepiolite and $Ti(OH)_4$ and investigation of new properties generated over physical mixture of $Ti(OH)_4$–sepiolite, Appl. Surf. Sci. 221 (2004) 167–177.
[32] A.M. Salem, M. Soliman Selim, Structure and optical properties of chemically deposited Sb_2S_3 thin films, J. Phys. D: Appl. Phys. 34 (2001) 12–17.